

Phytoplankton community structure, as derived from pigment signatures, in the Kuroshio Extension and adjacent regions in winter and spring

Yuta Nishibe¹ · Kazutaka Takahashi¹  · Mitsuhide Sato¹ · Taketoshi Kodama² · Shigeo Kakehi³ · Hiroaki Saito^{3,4} · Ken Furuya¹

Received: 6 October 2016 / Revised: 16 January 2017 / Accepted: 7 February 2017 / Published online: 23 February 2017
© The Oceanographic Society of Japan and Springer Japan 2017

Abstract The relationships between the spatiotemporal variation in phytoplankton community structure and environmental variables were investigated in the Kuroshio Extension (KE) region from winter to spring by analysing biomarker pigments. In winter, when the mixed layer was deep, phytoplankton communities were characterised by low biomass and a relatively high dominance of cryptophytes, followed by chlorophytes and pelagophytes. In spring, phytoplankton biomass generally increased with shoaling of the mixed layer. In April, when nitrate was not exhausted, chlorophytes became the most dominant group throughout the KE region, followed by cryptophytes. In May, in the south of the KE, phytoplankton biomass decreased with the depletion of nitrate and cyanobacteria dominated, whereas at the northern edge of the KE, phytoplankton biomass remained high. A predominance of diatoms occurred sporadically at the northern edge of the first ridge with a shallow mixed layer and an elevated nutrient. In contrast, the contribution of diatoms was low at the northern edge of the second ridge, despite high levels

of nitrate and silicic acid, suggesting that factors other than macronutrient depletion limited diatom production. In general, the contribution of diatoms to the total phytoplankton biomass in the KE region was small in both winter (2.9%) and spring (16%). This study showed that the phytoplankton communities in the KE region during the spring bloom were generally composed of non-diatom phytoplankton groups, chlorophytes, cryptophytes, and prasinophytes. It is necessary to identify the roles of non-diatoms in grazing food chains to more accurately evaluate the KE as a nursery area for pelagic fish.

Keywords HPLC · Phytoplankton community · Kuroshio Extension · Spring bloom

1 Introduction

The Kuroshio Extension (KE) and its adjacent regions are important nursery grounds for small pelagic fishes during winter and spring (Watanabe 2007). Food availability in these regions may be one of the factors that affect fluctuations in the populations of these fishes (Takahashi et al. 2008). Copepods, including their nauplii, are the main prey of larval fish (Nakata 1988, Nakata et al. 1995). Thus, the productivity of large phytoplankton, the preferred prey of copepods, is a key determinant of the recruitment success of these fishes. However, Nishibe et al. (2015) revealed that the contribution of small phytoplankton (<10 µm) to total phytoplankton biomass and primary production was generally higher than that of large phytoplankton (>10 µm) across the KE during spring bloom. They suggested that the growth of diatoms, which dominate in communities of large phytoplankton, is regulated by low concentrations of silicic acid and possibly iron in the KE region, in

Electronic supplementary material The online version of this article (doi:10.1007/s10872-017-0415-3) contains supplementary material, which is available to authorized users.

✉ Kazutaka Takahashi
akazutak@mail.ecc.u-tokyo.ac.jp

- ¹ Department of Aquatic Bioscience, The University of Tokyo, Tokyo, Japan
- ² Japan Sea National Fisheries Research Institute, Japan Fisheries Research and Education Agency, Niigata, Japan
- ³ Tohoku National Fisheries Research Institute, Japan Fisheries Research and Education Agency, Miyagi, Japan
- ⁴ Present Address: Atmosphere and Ocean Research Institute, The University of Tokyo, Chiba, Japan

addition to nitrate limitation. Despite the fact that primary production in the KE is dominated by small phytoplankton ($<10\ \mu\text{m}$), productivity may be as high as that of the slope water of the Kuroshio in spring, when large phytoplankton dominate total primary production (Nishibe et al. 2015). These results indicate that the KE region may have a phytoplankton community during spring bloom which is different from that in the slope water of the Kuroshio.

Since the KE is part of the western boundary current extension of a subtropical gyre propagating eastwards off the main island of Japan, the succession of the phytoplankton community of this region depends on its physical environment, namely, the vertical and lateral mixing processes of the subtropical Kuroshio, subpolar Oyashio, and coastal water masses, which in turn control the nutrient supply, light environment and phytoplankton species composition. The northwards and southwards convex parts of the meander are called ridges and troughs (Fig. 1b and d), respectively, and are numbered consecutively from west

to east (Qiu and Chen 2005; Nishibe et al. 2015). Clayton et al. (2014) conducted a fine-scale observation of the phytoplankton community structure across the KE front of the first ridge in autumn (October) and found differences between the phytoplankton communities in the oligotrophic subtropical and nutrient-rich subpolar water masses, which are largely distributed in the south and north of the front, respectively. However, the spatial distribution of the phytoplankton communities near the front is influenced by the intrusion of the southern warmer water into the north as a warm filament (Clayton et al. 2014) and the transportation of the coastal (Marumo 1967; Clayton et al. 2017) and Oyashio water masses (Yamamoto et al. 1988; Clayton et al. 2014). A high abundance of diatoms was observed in the low-salinity Oyashio water mass at the sea surface in the vicinity of the northern edge of the first ridge of the KE (Clayton et al. 2014). Similarly, the highest abundance of diatoms was observed in spring at the northern edge of the first ridge (Marumo et al. 1961; Yamamoto et al. 1988),

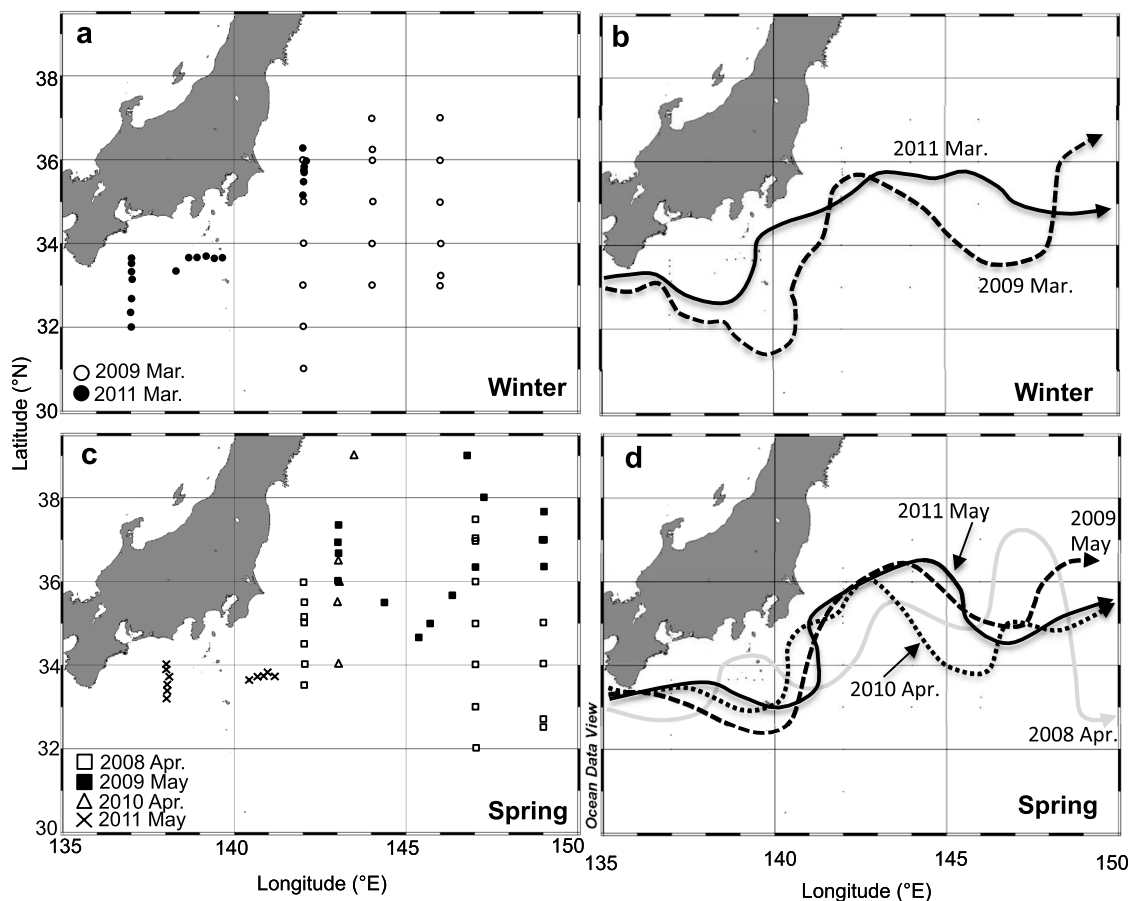


Fig. 1 Sampling stations and flow paths of the Kuroshio and the Kuroshio Extension in the study sites in **a**, **b** winter and **c**, **d** spring from 2008 to 2011. Flow paths were drawn based on the Quick Bulletin of Ocean Conditions issued by the Japan Coast Guard ([http://](http://www1.kaiho.mlit.go.jp/KANKYO/KAIYO/qboc/)

www1.kaiho.mlit.go.jp/KANKYO/KAIYO/qboc/) except for April 2008, when the position of the first ridge was revised based on physical observations made during cruises

where primary production is enhanced due to shoaling of the mixed layer caused by distribution of the warmer southern water in the cold northern water (Nishibe et al. 2015). Yamamoto et al. (1988) found a dominance of small phytoplankton (<10 μm) across the KE in the vicinity of the first ridge, with an increase in the contribution of large phytoplankton (>10 μm) in the north of the temperature front. On the other hand, small phytoplankton (<10 μm), especially picophytoplankton (<2 μm), were reportedly dominant across the KE in the vicinity of the second ridge in spring (Odate and Maita 1988). These studies indicate that the occurrence of a large phytoplankton community mainly consisting of diatoms seems to be limited to the frontal area of the KE, and small phytoplankton groups are dominant in the other areas, although the taxonomic composition of small phytoplankton—which also affects copepod production (Calbet et al. 2000)—has not been investigated in detail (Clayton et al. 2017).

To understand the ecological significance of the KE as a nursery ground for pelagic fish, the distribution and succession of the phytoplankton community during spring bloom, which coincides with their recruitment season (Noto and Yasuda 2003; Yatsu et al. 2005; Takasuka et al. 2007; Watanabe 2007), must be investigated in detail with extensive spatial coverage so that the regional characteristics of the KE are clarified. Therefore, the study reported in the present paper attempted to reveal the entire phytoplankton community structure in the vicinity of the KE in winter and spring and to relate that structure to environmental conditions by analyzing phytoplankton pigments, which is necessary to clarify the biomass and the relative contribution of algal taxa.

2 Materials and methods

Hydrographic surveys and water sampling were conducted at 90 stations near the KE and Kuroshio in winter and spring between 2008 and 2011 (Fig. 1), during 6 cruises of R/V *Wakataka-maru* (Japan Fisheries Research and Education Agency), R/V *Shoyo-maru* (Fisheries Agency), R/V *Hakuho-maru*, and R/V *Tansei-maru* (JAMSTEC). A SBE 9plus CTD (Sea-Bird Electronics) with a fluorometer (Wetlabs) was used to obtain temperature, salinity, and chlorophyll fluorescence profiles. Underwater light intensity was measured with a PNF (profiling natural fluorescence) radiometers (Biospherical). Using acid-cleaned Niskin bottles mounted on a CTD carousel system, water samples were collected from a depth of 10 m in winter and spring, and from the subsurface chlorophyll *a* maximum (SCM) in spring. They were also collected from depths corresponding to 50, 25, 10, 5, and 1% light intensity just beneath the surface as well as from the surface itself using a bucket at

stations where primary production was measured (Nishibe et al. 2015). Two-litre water samples were filtered through Whatman GF/F filters under gentle suction (<0.02 MPa), and the filters were maintained at $-80\text{ }^{\circ}\text{C}$ until analysis was performed on land.

In a laboratory, the filters were completely broken apart by sonication (Sonifier 150, Branson) in 3.5 mL of 95% methanol, and pigments were extracted in the dark at $4\text{ }^{\circ}\text{C}$ for 3 h. The extracts were filtered through a 0.2- μm PTFE syringe filter and then 1.6 mL extracts were injected into a HPLC (high-performance liquid chromatography) system after being mixed with 0.4 mL ultrapure water. Pigments were eluted based on a high-pressure mixing protocol described by Zapata et al. (2000). During the analysis, a 150-mm reversed-phase C_8 column with a pore size of 3.5 μm (GL Science) was maintained at $25\text{ }^{\circ}\text{C}$. Pigments were detected by a photodiode array UV–Vis detector (SPD-M10AV, Shimadzu) with a spectral resolution of 1.2 nm. Pigments were identified and quantified by referring their retention times, absorption spectra, and peak areas to those of standards (Danish Hydraulic Institute).

The relative contribution of algal taxa was estimated from concentrations of biomarker pigments using the CHEMTAX calculation (Mackey et al. 1996), as performed with the CHEMTAX v.1.95 software. Diatoms, dinoflagellates, haptophytes, pelagophytes, cryptophytes, chlorophytes, prasinophytes, cyanobacteria, and *Prochlorococcus* were chosen for phytoplankton groups in the initial ratio matrix. This was based on previous reports of their occurrence in the vicinity of the KE (Thronsen 1983; Kok et al. 2012a, b, 2014) and our preliminary survey (data not shown) in the vicinity of the KE and the Kuroshio in winter and spring (Table 1). Fucoxanthin (“Fuco”), peridinin (“Perid”), 19'-hexanoyloxyfucoxanthin (“Hex”), 19'-butanoyloxyfucoxanthin (“But”), diadinoxanthin (“Diad”), alloxanthin (“Allo”), violaxanthin (“Viola”), prasinoxanthin (“Pras”), zeaxanthin (“Zea”), chlorophyll *b* (“Chl *b*”), divinyl chlorophyll *a* (“DV Chl *a*”), and monovinyl chlorophyll *a* (“Chl *a*”) were used as the biomarker pigments in the initial ratio matrix. Ratios of the biomarker pigments to Chl *a* or DV Chl *a* in each phytoplankton group were derived using methods from Miki et al. (2008). In the following description, the total Chl *a* is the sum of the Chl *a* and DV Chl *a* concentrations. Since phytoplankton adjust their intracellular pigment concentrations according to light availability (Mackey et al. 1998), phytoplankton taxonomic compositions were estimated separately for samples taken at depths >30 m and ≤ 30 m (generally corresponding to the upper and lower parts of the euphotic zone, respectively) via CHEMTAX calculations. In the CHEMTAX calculations, we adopted the method of Mackey et al. (1996), in which the CHEMTAX calculation was performed only once and the phytoplankton groups roughly corresponded

Table 1 Initial ratios of biomarker pigments to chlorophyll *a* (w/w) in the CHEMTAX calculations performed in this study

	Fuco	Perid	Hex	But	Diad	Allo	Viola	Pras	Zea	Chl <i>b</i>	DV Chl <i>a</i>	Chl <i>a</i>
Diatoms	0.75	0	0	0	0.14	0	0	0	0	0	0	1
Dinoflagellates	0	1.1	0	0	0.24	0	0	0	0	0	0	1
Prymnesiophytes	0	0	1.7	0	0.10	0	0	0	0	0	0	1
Pelagophytes	0.35	0	0	0.76	0.19	0	0	0	0	0	0	1
Cryptophytes	0	0	0	0	0	0.23	0	0	0	0	0	1
Chlorophytes	0	0	0	0	0	0	0.06	0	0.01	0.26	0	1
Prasinophytes	0	0	0	0	0	0	0.06	0.32	0	0.95	0	1
Cyanobacteria	0	0	0	0	0	0	0	0	0.35	0	0	1
<i>Prochlorococcus</i>	0	0	0	0	0	0	0	0	0.32	1.1	1	0

to the class level, for the following reason: the cell-specific chlorophyll *a* content of cyanobacteria estimated from successive calculations (Latasa 2007) was considerably lower than the general value previously reported for the study area (1.0–1.4 fg cell⁻¹; Hashihama et al. 2008), while the cell-specific chlorophyll *a* content estimated using a single iteration was closer to the reported value (see Fig. S1a, b in the Electronic supplementary material, ESM). The estimated phytoplankton communities at a depth of 10 m in winter and spring and at the SCM in spring were clustered based on the biomass (Chl *a* or DV Chl *a* concentration) of each algal taxon using a group average method employing Bray–Curtis similarity (PRIMER v6, PRIMER-E Ltd, Plymouth, UK) (Clarke and Gorley 2006). Vertical taxonomic compositions were estimated at the stations where primary production was measured (Nishibe et al. 2015).

Samples for nutrient analysis were maintained at –20 °C, and concentrations of nitrate, silicic acid, and phosphate were measured colourimetrically in a laboratory on land using an autoanalyser (TRAACS2000, Bran+Luebbe, UK) (Hansen and Koroleff 1999). Concentrations of ammonium were also measured during the spring cruises. Mixed-layer depth (hereafter, MLD) was defined as the depth where sigma- θ increased by 0.125 from its value at a depth of 10 m (Levitus 1982). Relationships between the environmental parameters and phytoplankton community types, as determined from the cluster analysis, were analysed using principal component analysis (PCA) diagrams (PRIMER v.6). In the PCA analysis, each environmental parameter was normalised and then log(*X*) and log(*Y* + 1) transformations were performed for the MLD, the SCM (*X* m), and nutrient (nitrate, phosphate, silicic acid, and ammonium) concentrations (*Y* μ M) (Clarke and Gorley 2006).

Indicative temperatures of the KE (14 °C) and Kuroshio (15 °C) axes at a depth of 200 m (Kawai 1972) were applied to assign the stations to distinct water masses that vary across the KE or Kuroshio axes. Moreover, stations near the KE were distinguished based on temperature at a depth of 10 m into those in the KE region (>17 °C) and

those in the Kuroshio–Oyashio transition region (<17 °C, hereafter “transition region”) according to Nishibe et al. (2015).

3 Results

3.1 CHEMTAX calculation

Ratios of biomarker pigments to Chl *a* or DV Chl *a* in the final ratio matrices did not vary drastically from those in the initial ratio matrix, except that the ratio of Chl *b* to Chl *a* of prasinophytes in winter doubled (Tables 1, 2). The final ratios of photosynthetic accessory pigments of Fuco of diatoms and Pras and Chl *b* of prasinophytes showed higher values in samples taken at depths of ≤ 30 m than >30 m (Table 2b, c). On the other hand, the final ratios of photoprotective pigments of Diad of pelagophytes, Viola of chlorophytes and Zea of cyanobacteria showed higher values in samples taken at depths >30 m than in those taken at ≤ 30 m. Variations in the ratios of the other biomarker pigments with respect to Chl *a* or DV Chl *a* in the final ratio matrices was small between samples taken at depths >30 m and those taken at ≤ 30 m. Significant positive correlations were observed between Chl *a* concentrations of cyanobacteria and cell densities of *Synechococcus* and between Chl *a* concentrations and cell densities of cryptophytes, as measured using flow cytometry ($p < 0.05$, *t* test; Fig. S1 in the ESM).

3.2 Phytoplankton community structure in relation to environmental conditions in winter and spring

In the clustering analysis, during each season and at each sampling depth, stations were divided into several groups according to appropriate levels of similarity (>ca. 50%) in their phytoplankton communities. Phytoplankton communities at depths of 10 m in winter were clustered into two groups (WH and WL) based on a similarity of 60%

Table 2 Final ratios of biomarker pigments to chlorophyll *a* (w/w) in the CHEMTAX calculations performed in this study

	Fuco	Perid	Hex	But	Diad	Allo	Viola	Pras	Zea	Chl <i>b</i>	DV Chl <i>a</i>	Chl <i>a</i>
(a) Winter												
Diatoms	0.98	0	0	0	0.11	0	0	0	0	0	0	1
Dinoflagellates	0	1.1	0	0	0.24	0	0	0	0	0	0	1
Prymnesiophytes	0	0	1.6	0	0.12	0	0	0	0	0	0	1
Pelagophytes	0.35	0	0	0.76	0.07	0	0	0	0	0	0	1
Cryptophytes	0	0	0	0	0	0.27	0	0	0	0	0	1
Chlorophytes	0	0	0	0	0	0	0.06	0	0.01	0.26	0	1
Prasinophytes	0	0	0	0	0	0	0.09	0.52	0	1.9	0	1
Cyanobacteria	0	0	0	0	0	0	0	0	0.35	0	0	1
<i>Prochlorococcus</i>	0	0	0	0	0	0	0	0	0.32	1.1	1	0
(b) Above 30 m depth in spring												
Diatoms	0.88	0	0	0	0.11	0	0	0	0	0	0	1
Dinoflagellates	0	1.1	0	0	0.24	0	0	0	0	0	0	1
Prymnesiophytes	0	0	1.7	0	0.10	0	0	0	0	0	0	1
Pelagophytes	0.35	0	0	0.76	0.19	0	0	0	0	0	0	1
Cryptophytes	0	0	0	0	0	0.27	0	0	0	0	0	1
Chlorophytes	0	0	0	0	0	0	0.04	0	0.01	0.26	0	1
Prasinophytes	0	0	0	0	0	0	0.06	0.32	0	0.95	0	1
Cyanobacteria	0	0	0	0	0	0	0	0	0.87	0	0	1
<i>Prochlorococcus</i>	0	0	0	0	0	0	0	0	0.32	1.1	1	0
(c) At and below 30 m depth in spring												
Diatoms	1.1	0	0	0	0.08	0	0	0	0	0	0	1
Dinoflagellates	0	1.1	0	0	0.24	0	0	0	0	0	0	1
Prymnesiophytes	0	0	1.6	0	0.10	0	0	0	0	0	0	1
Pelagophytes	0.35	0	0	0.76	0.03	0	0	0	0	0	0	1
Cryptophytes	0	0	0	0	0	0.26	0	0	0	0	0	1
Chlorophytes	0	0	0	0	0	0	0.02	0	0.01	0.26	0	1
Prasinophytes	0	0	0	0	0	0	0.06	0.46	0	1.4	0	1
Cyanobacteria	0	0	0	0	0	0	0	0	0.73	0	0	1
<i>Prochlorococcus</i>	0	0	0	0	0	0	0	0	0.32	1.1	1	0

(Fig. 2a). The first group, WH, was characterised by a higher total Chl *a* ($0.37 \pm 0.090 \mu\text{g L}^{-1}$, $n = 26$) than the other group, WL ($0.16 \pm 0.026 \mu\text{g L}^{-1}$, $n = 12$) (Fig. 2a; Table 3). The most dominant group was cryptophytes in both WH and WL, accounting for 24–25% of the total Chl *a*. Chlorophytes (16%), and pelagophytes (15%) were subdominant in WH, while the relative importance of pelagophytes (21%) was higher in WL, followed by prymnesiophytes (17%). The contribution of diatoms to total Chl *a* was small (<11%) in both WH and WL (Fig. 2a). In the vicinity of the KE, WH and WL were generally distributed in the north and the south of the KE, respectively (Fig. 3). However, WH was also observed in the south of the KE and near the cold core ring along 142°E in 2009 (Fig. 3a). In the vicinity of the Kuroshio, WH was distributed in the north of the Kuroshio and only along 137°E in the south of the Kuroshio (Fig. 3b). In contrast with the KE region, WL was observed to the north of the Kuroshio axis (Stns. 1 and

10). Throughout the study sites, WH was observed under a wider range of environmental conditions than WL (Fig. 4). In general, WH was associated with lower temperatures and salinity, a shallower MLD and higher nutrient concentrations than WL (Table 3).

In spring, the communities were clustered into five groups (SH1, SH2, SH3, SL1, and SL2), each of showed any intragroup similarity of 52% at depths of 10 m (Fig. 2b). Three of those groups had a high total Chl *a* (SH1: $0.54 \pm 0.21 \mu\text{g L}^{-1}$, $n = 29$; SH2: $0.69 \pm 0.13 \mu\text{g L}^{-1}$, $n = 6$; SH3: $0.62 \mu\text{g L}^{-1}$) and two groups had a low total Chl *a* (SL1: $0.24 \pm 0.034 \mu\text{g L}^{-1}$, $n = 7$; SL2: $0.18 \pm 0.043 \mu\text{g L}^{-1}$, $n = 8$) (Fig. 2b; Table 3). The flow path of the KE was variable in 2008–2010 (Fig. 5). Large fluctuations in the meander of the KE were observed in April 2008, and the first ridge formed near 147°E at a high latitude of ca. 38°N (Fig. 5a). In contrast, the meander of the KE was rather stable in April 2010 and May

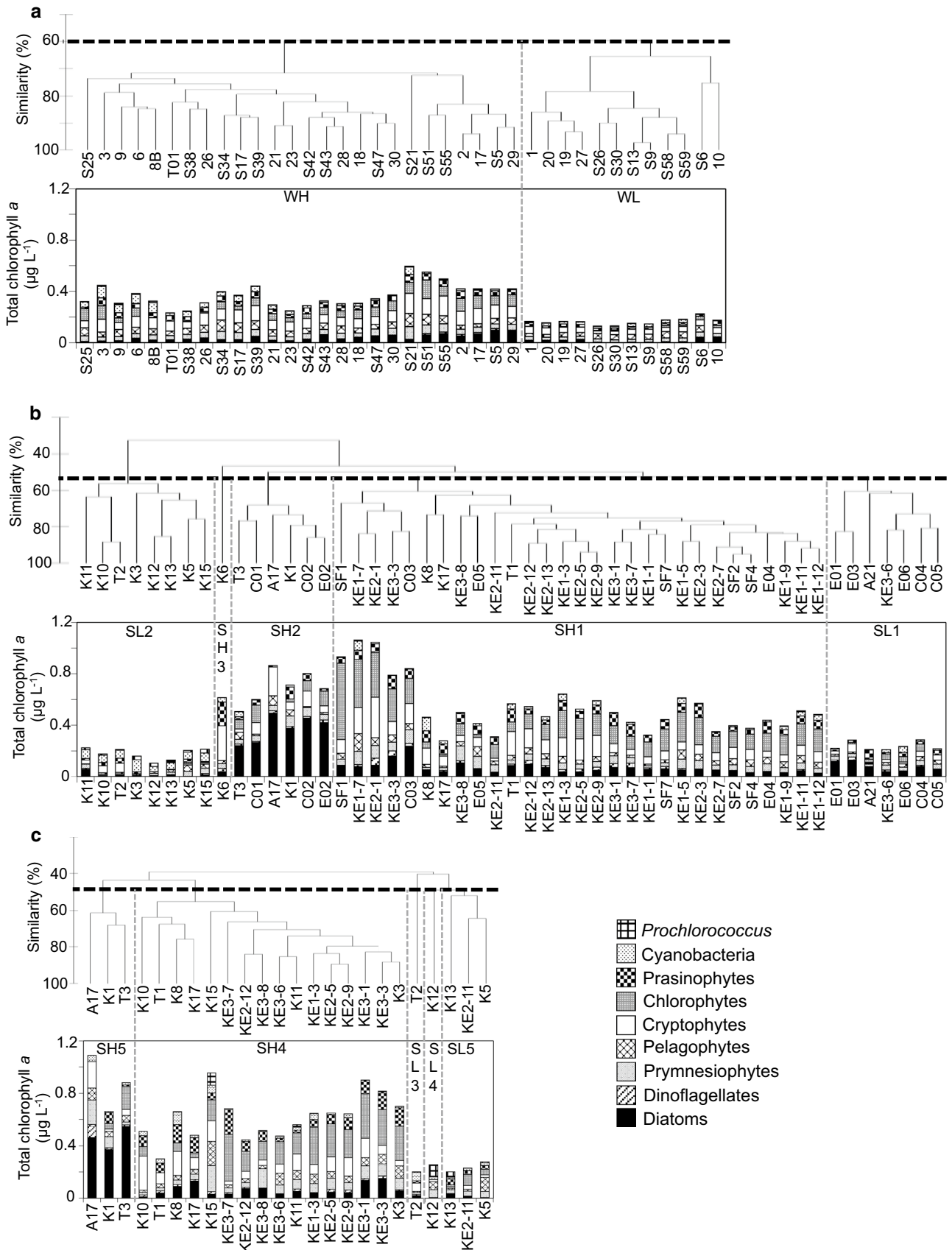


Fig. 2 Phytoplankton community structure near the Kuroshio Extension and Kuroshio at a depth of 10 m in **a** winter and **b** spring, and **c** depths of the subsurface chlorophyll *a* maximum in spring. Phytoplankton communities were clustered into two groups (WH and WL) based on a similarity of 60% in **a**, five groups (SL2, SH3, SH2, SH1, and SL1) based on a similarity of 52% in **b**, and five groups (SH5, SH4, SL3, SL4, and SL5) based on a similarity of 49% in **c**

2009, and the first ridge formed near 144°E at relatively low latitude of 36.5°N (Fig. 5b, d). Near the KE in April 2008 and 2010, phytoplankton communities were characterised by a uniform distribution of SH1 (Fig. 5a, b). Chlorophytes and cryptophytes were the most dominant and subdominant groups, respectively (Fig. 2b), except at Stn. KE3-6 south of the first trough (Fig. 5a), where the community was categorised as SL1, with no particular dominant phytoplankton group (Fig. 2b). In the Kuroshio region in April, various types of phytoplankton communities were observed (Fig. 5c). Whereas SH1 was distributed near the Kuroshio axis (Stns. C03, E04, and E05), SH2 (in which diatoms dominated, and there was a high total Chl *a*) was observed in the inshore areas of the Kuroshio (Stns. C01, C02, and E02). Here, the dominance of diatoms with a low total Chl *a* (SL1) was also observed at Stns. E01 and E03 (Figs. 2b, 5c), though the same community was also found in the south of the Kuroshio (Stns. E06, C04, and C05). In May of 2009, a distinct distribution pattern of communities with a high total Chl *a* was observed to the north and those with a low total Chl *a* to the south in the vicinity of the KE (Fig. 5d). A community dominated by diatoms was observed sporadically at the northern edge of the first ridge (Stn. T3) in the KE region as well as in the north of the second ridge (Stn. K1), and by a warm core ring (Stn. A17) in the transition region (Fig. 5d). Unlike in April, the occurrence of SH1 was restricted to the northern edge of the KE (Stns. K17, K8, and T1) in May (Fig. 5a, b, d). Dominant groups of SH1 changed from chlorophytes (April) to cryptophytes, followed by prasinophytes (Stns. K17 and T1) and cyanobacteria (Stn. K8) (Fig. 2b). In addition, SH3, in which cryptophytes and prasinophytes were the dominant groups, was observed north of the first trough of the KE at Stn. K6. In the south of the KE, phytoplankton communities—predominantly cyanobacteria (SL2)—characterised by low biomass were found between the first and second ridges. Generally, phytoplankton communities with a low total Chl *a* (SL1 and SL2) were observed at stations with higher temperatures and lower nutrient concentrations (Fig. 6; Table 3). On the other hand, phytoplankton communities with a high total Chl *a* (SH1, SH2, and SH3) were not associated with specific environmental parameters (Fig. 6; Table 3). SH1 was generally observed at high temperatures (19.5 ± 1.3 °C) and relatively low nitrate concentrations

(0.63 ± 0.49 μM). Communities dominated by diatoms (SH2) occurred at three stations in different regions: two stations were in the transition region (Stns. A17 and K1) and the other station (Stn. T3), which had a relatively high temperature, was at the northern edge of the first ridge (Fig. 5d). The community that was dominated by cryptophytes and prasinophytes but lacked chlorophytes (SH3) was associated with a relatively low temperature (17.3 °C) and a depleted nitrate concentration (<0.1 μM). SH2 and SH3 were observed in environments with a shallower MLD compared with the environments associated with SH1 (Fig. 6; Table 3).

In spring, the formation of the SCM was observed at 50% and 88% of the stations during the WK0804 (April 2008) and WK0905 cruises (May 2009), respectively (Fig. 7). The depth of the SCM ranged from 20 to 80 m, and was deeper in the south of the KE than in the north (data not shown). Phytoplankton communities at the SCM were clustered into two groups with a high total Chl *a* (SH4: 0.62 ± 0.17 μg L⁻¹, *n* = 16; SH5: 0.88 ± 0.21 μg L⁻¹, *n* = 3), and three groups with a low total Chl *a* (SL3: 0.20 μg L⁻¹; SL4: 0.25 μg L⁻¹; SL5: 0.24 ± 0.038 μg L⁻¹, *n* = 16), based on a similarity of 49% (Fig. 2c; Table 3). Phytoplankton compositions in SH4 and SH5 were similar to those in SH1 and SH2, respectively (Fig. 2b, c). In April, near the KE, a high total Chl *a* group of SH4 in which chlorophytes (30%) were the most dominant, followed by cryptophytes (17%) and prasinophytes (15%), dominated communities at SCM. Stn. KE2-11 was an exception, with a low total Chl *a* (SL5) in the south of the KE along 147°E (Figs. 2c, 7a). In May, phytoplankton communities with a high and a low total Chl *a* were distributed in the north and south of the KE, respectively, as observed at a depth of 10 m. At stations where diatoms were dominant at 10 m (SH2), they were also predominant at the SCM (SH5) (Figs. 5d, 7b). In the south of the KE in May, phytoplankton communities with a high total Chl *a* were only found at the SCM (Stns. K3, K10, K11, and K15), while those at 10 m depth at the same station were classified as a community with low total Chl *a* (SL2) (Figs. 5d, 7b). Communities with low total Chl *a*, in which *Prochlorococcus* (36%) and pelagophytes (23%) were dominant (SL4), were observed in the south of the first ridge (Stn. K12), while those dominated by cyanobacteria (32%) and cryptophytes (31%) (SL3) occurred at the northern edge of the first trough (Stn. T2). Although communities with a high total Chl *a* (SH4 and SH5) were observed in environments with high nitrate concentrations and low temperatures, those with a low total Chl *a* (SL3, SL4, and SL5) were found in areas with low nitrate concentrations and high temperatures (Fig. 8; Table 3).

Table 3 Phytoplankton community types and associated environmental parameters in the vicinity of the Kuroshio Extension and the Kuroshio in winter and spring

Season	Sampling layer	Depth (m)	Phytoplankton community type	Total chlorophyll <i>a</i> ($\mu\text{g L}^{-1}$)	Dominant phytoplankton groups (%)	Temperature ($^{\circ}\text{C}$)	Salinity	Mixed layer depth (m)	Nitrate (μM)	Silicic acid (μM)
Winter	Surface	10	WH	0.37 \pm 0.09	CP (25) CL (16)	16.7 \pm 3.4	34.57 \pm 0.24	100 \pm 67	3.5 \pm 2.8	5.9 \pm 4.4
		10	WL	0.16 \pm 0.03	CP (24) PL (21)	18.4 \pm 1.4	34.69 \pm 0.04	130 \pm 76	2.0 \pm 1.7	3.2 \pm 3.0
Spring	Surface	10	SH1	0.54 \pm 0.21	CL (31) CP (19)	19.5 \pm 1.3	34.69 \pm 0.06	86 \pm 80	0.63 \pm 0.49	2.4 \pm 0.50
		10	SH2	0.69 \pm 0.13	DT (54) CP (14)	16.3 \pm 2.7	34.49 \pm 0.24	27 \pm 8	1.4 \pm 0.9	3.7 \pm 2.0
		10	SH3	0.62	CP (44) PS (30)	17.3	34.47	21	0.033	3.2
		10	SL1	0.24 \pm 0.03	DT (31) PM (13)	18.4 \pm 2.3	34.70 \pm 0.14	49 \pm 26	0.79 \pm 1.6	3.2 \pm 3.0
		10	SL2	0.18 \pm 0.04	CY (35) PM (12)	20.8 \pm 1.1	34.64 \pm 0.04	35 \pm 14	0.01 \pm 0.02	2.0 \pm 0.42
	SCM	31 \pm 8	SH4	0.62 \pm 0.17	CL (30) CP (17)	18.7 \pm 1.4	34.67 \pm 0.08	33 \pm 11	1.1 \pm 1.1	3.6 \pm 1.5
		22 \pm 3	SH5	0.88 \pm 0.21	DT (52) PM (11)	15.6 \pm 4.0	34.33 \pm 0.26	25 \pm 5	2.3 \pm 1.8	4.1 \pm 2.8
		30	SL3	0.20	CY (32) CP (31)	19.2	34.61	27	0.0048	3.0
		60	SL4	0.25	PR (36) PL (23)	20.6	34.68	57	0	1.8
		60 \pm 17	SL5	0.24 \pm 0.04	CL (20) PL (19)	18.9 \pm 0.9	34.73 \pm 0.06	54 \pm 34	0.34 \pm 0.19	2.3 \pm 0.33

CP cryptophytes, CL chlorophytes, PL pelagophytes, PS prasinophytes, DT diatoms, CY cyanobacteria, PM prymnesiophytes, PR *Prochlorococcus*

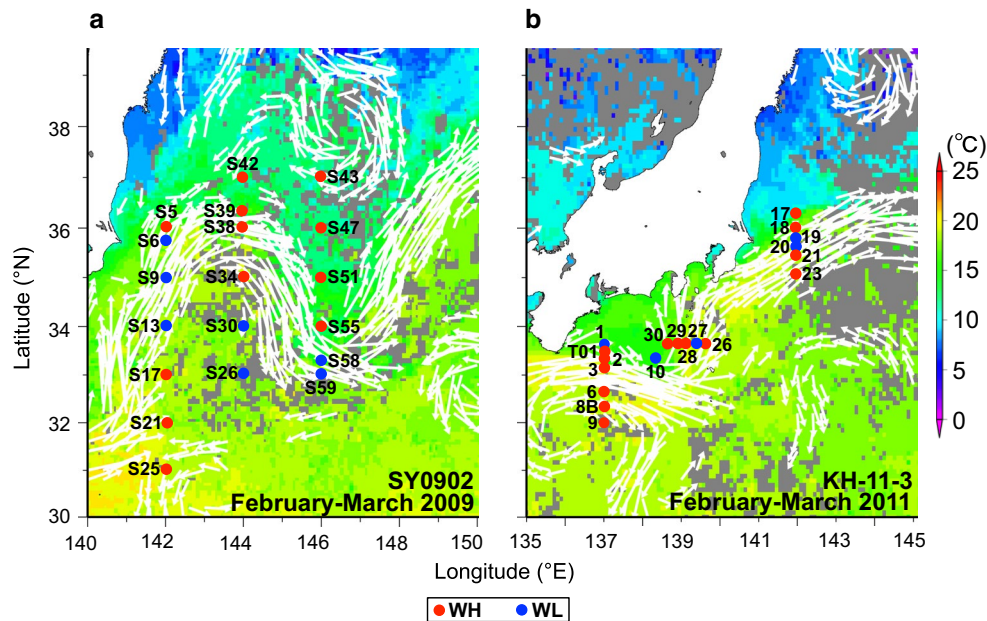


Fig. 3 Distribution of winter phytoplankton community types at a depth of 10 m identified from cluster analysis during the **a** SY0902 and **b** KH-11-3 cruises (red solid circles WH; blue solid circles WL). Geostrophic currents, denoted by white arrows, were calculated from the absolute dynamic topography derived from the merged products

of the Jason-1, Jason-2, GFO, and Envisat satellite altimeters and were overlaid on level-3 SST ($^{\circ}\text{C}$) images with 9-km resolution from MODIS/aqua (<http://oceancolor.gsfc.nasa.gov/>), which were composited for 7 days around the middle of the period of each cruise (color figure online)

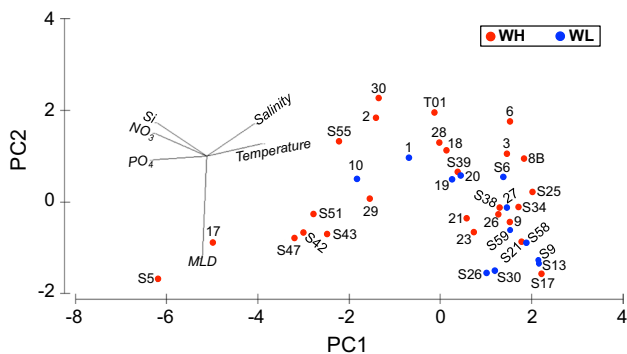


Fig. 4 Relationships between environmental parameters and phytoplankton communities at a depth of 10 m in winter (red solid circles WH; blue solid circles WL) in a PCA diagram (color figure online)

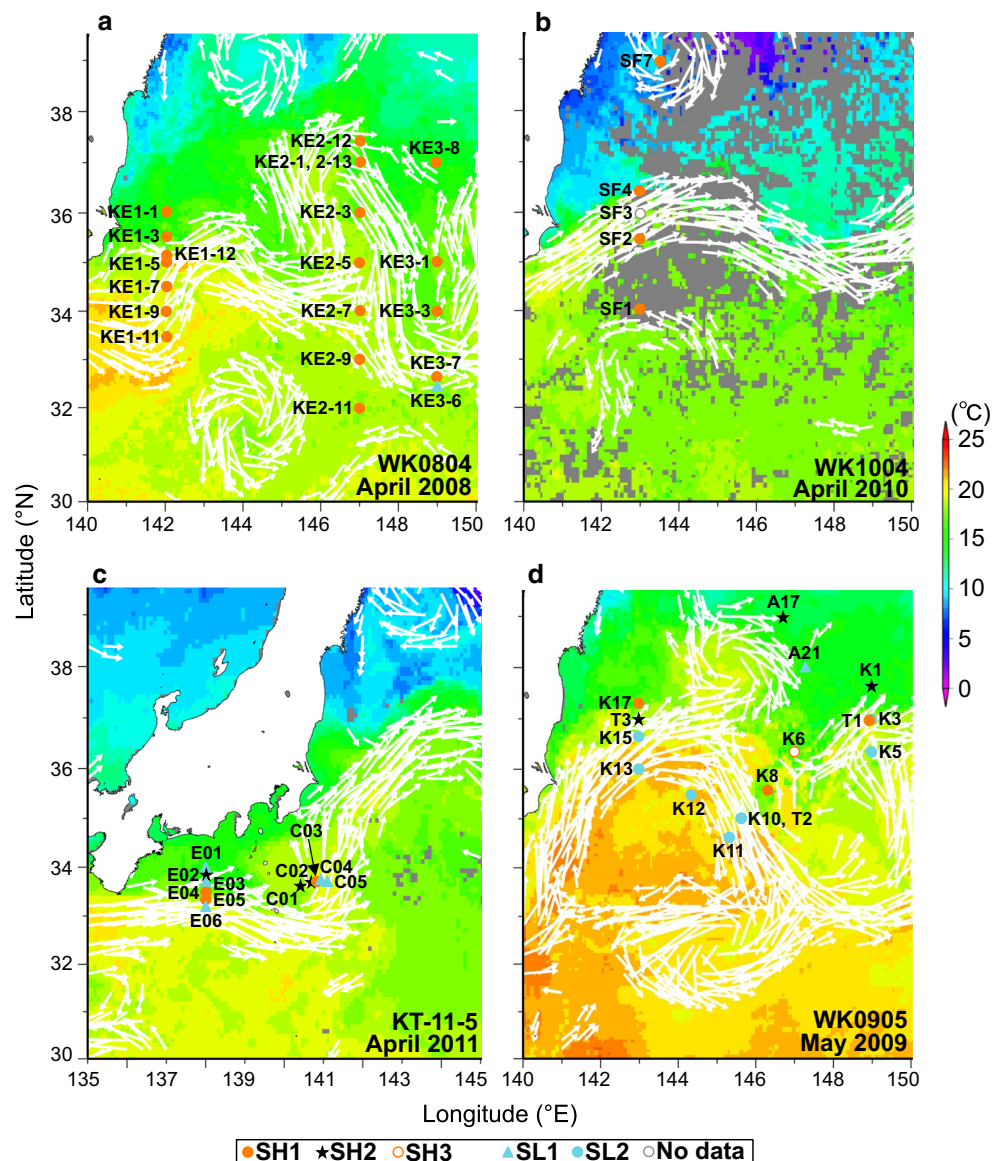
3.3 Vertical distributions of phytoplankton

Vertical structures of phytoplankton communities in winter were determined for four stations with WH and three stations with WL (Fig. 9a). In general, total Chl *a* and relative contributions of algal taxa did not show distinct vertical variations, and a slight elevation of total Chl *a* was accompanied by an increase in the contribution of chlorophytes in the euphotic zone regardless of community type. Exceptions were found at some stations with WL. For instance, at Stn. S6 just south of the axis of the first ridge of the KE,

total Chl *a* decreased at the bottom of the euphotic zone, coinciding with a decrease and an increase in the contributions of diatoms and pelagophytes, respectively. At Stn. S59 south of the first trough, although total Chl *a* was vertically uniform throughout the euphotic zone, an increase in the contribution of diatoms was observed with a decrease in the contribution of pelagophytes in the upper euphotic zone.

In spring, vertical structures of phytoplankton communities were investigated for seven stations with SH1, two stations with SH2, and one station each with SL1 and SL2 (Fig. 9b). Compared with winter, vertical distribution patterns of total Chl *a* in the euphotic zone varied widely among stations, and the contribution of algal taxa generally depended on the total Chl *a*. Firstly, total Chl *a* was higher in the upper euphotic zone at Stns. KE2-13, KE1-11, KE1-12, SF3, and T1 with SH1 and at Stn. C02 with SH2. At Stn. KE2-13 (near the axis of the first ridge of KE), which was dominated by chlorophytes followed by cryptophytes, the contribution of cryptophytes decreased while that of pelagophytes increased with the decrease in total Chl *a* close to the bottom of the euphotic zone. At Stns. KE1-11, KE1-12, and SF3 (south of the first ridge of KE), where chlorophytes dominated, the contribution of algal taxa was almost unchanged in the euphotic zone. At Stn. T1 (the northern edge of the second ridge), where cryptophytes and prasinophytes were the dominant groups, a decrease

Fig. 5 Distribution of spring phytoplankton community groups at a depth of 10 m as identified from cluster analysis during the **a** WK0804, **b** WK1004, **c** KT-11-5, and **d** WK0905 cruises (orange solid circles SH1, black stars SH2, orange open circles SH3, light blue solid triangles SL1, light blue solid circles SL2). Geostrophic currents (white arrows) and SST images were derived in the same way as described for Fig. 3 (color figure online)



and an increase in the contributions of diatoms and cryptophytes, respectively, were observed in the upper euphotic zone. At Stn. C02 (inshore area of the Kuroshio) which was dominated by diatoms, their contribution increased slightly towards the bottom of the euphotic zone.

Secondly, a distinct SCM was formed in the upper (Stn. T3 (SH2)) and lower (Stns. KE3-7 (SH1) and T2 (SL2)) euphotic zones. At Stn. T3 (northern edge of the first ridge of the KE), the contribution of diatoms and chlorophytes was highest at and just below the SCM, respectively. At Stn. KE3-7 (south of the first trough of the KE), where chlorophytes and prasinophytes were dominant, the contribution of chlorophytes slightly increased toward the bottom of the euphotic zone, while that of prasinophytes was highest just above the SCM. At Stn. T2 (northern edge of the first trough of the KE), where cryptophytes and

prasinophytes were important groups, their contributions were almost unchanged in the euphotic zone, whereas those of cyanobacteria and chlorophytes increased near the sea surface and at the SCM, respectively.

Thirdly, the total Chl *a* slightly increased towards the bottom of the euphotic zone at Stn. KE3-8 with SH1. At Stn. KE3-8 (transition region), where diatoms, prymnesiophytes, and chlorophytes were important groups, the contribution of prymnesiophytes was almost unchanged vertically, while a decrease and an increase in the contributions of diatoms and chlorophytes, respectively, were observed toward the bottom of the euphotic zone.

Fourthly, total Chl *a* was uniform at Stn. E01 with SL1. At Stn. E01 (inshore area of the Kuroshio), where diatoms dominated, their dominance increased toward the bottom of the euphotic zone.

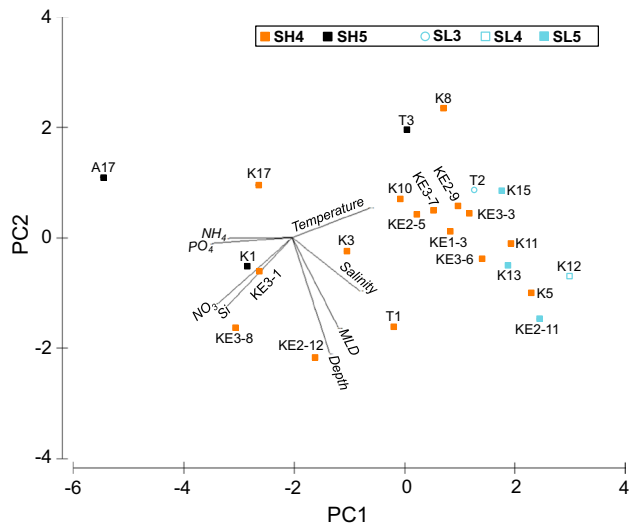


Fig. 8 Relationships between environmental parameters and phytoplankton communities at the depths of the subsurface chlorophyll *a* maximum in spring (orange solid squares SH4, black solid squares SH5, light blue open circles SL3, light blue open squares SL4, light blue solid squares SL5) in a PCA diagram (color figure online)

phytoplankton compositions during the spring bloom near the KE region.

In winter, the phytoplankton biomass was generally low. The phytoplankton biomass and compositions were uniform throughout the euphotic zone (Figs. 2a, 9a). During this period, most of the sampling stations were characterised by a deep MLD (Table 3) and nitrate and silicic acid were replete in the euphotic zone due to the winter convective mixing (Table 3; refer to Figures 3 and 4 in Nishibe et al. 2015). Total Chl *a* was slightly higher and the MLD shallower in the north of the KE and Kuroshio axes than in the south (Fig. 3; Table 3). Cryptophytes were the most dominant group throughout the study sites, followed by chlorophytes and pelagophytes in communities with high and low total Chl *a*, respectively. Although diatoms were generally a minor group in winter, their relative importance was slightly higher at some stations at the northern edges of the KE (Stns. S5 and 17) (Figs. 2a, 3). This was consistent with the results of a study by Kawarada et al. (1968), who found higher cell densities of diatoms at the northern edges and in the north of the KE, from the first ridge to the first trough, than in the surrounding areas in winter.

From winter to spring, phytoplankton biomass near the KE generally increased with shoaling of the MLD (Table 3). In conjunction with the increase in biomass, phytoplankton community compositions became more variable than in winter, indicating that community succession responded strongly to spatiotemporal variations in nutrients and light. In April, chlorophytes became the most dominant group, followed by cryptophytes, throughout the KE

region (Figs. 2b, c, 5a, b, 7a). This was consistent with the results of Hashihama et al. (2008), in which the predominance of chlorophytes and cryptophytes was associated with the flushing of the Kuroshio in Sagami Bay. In May, the phytoplankton biomass near the sea surface decreased with further MLD shoaling associated with nutrient consumption in the south of the KE, where cyanobacteria dominated (Figs. 2b, 5d; Table 3). Compared with April, the chlorophyll maximum layer shifted downwards, and a distinct SCM was formed south of the KE (Stns. K3, K10, K11 and K15), reflecting bloom succession associated with a decrease in nutrients at the surface layer (Figs. 2b, c, 5d, 7b). At the northern edge and in the north of the KE, the phytoplankton biomass remained high, with variable compositions (Fig. 5d). Communities with high phytoplankton biomass at the northern edge were dominated by cryptophytes, prasinophytes, cyanobacteria (Stns. K6, K8, K17, and T1), and diatoms (Stn. T3), and the contribution of chlorophytes decreased (Figs. 2b, 5d). Isada et al. (2009) reported a similar succession from chlorophytes to *Synechococcus* as nitrate consumption proceeded from winter to summer in the north of the KE in the transition region. In the KE region, the main primary producers during the spring bloom are small (<10 μm) phytoplankton, primarily due to the low availability of nitrate and silicic acid in winter. The formation of the spring bloom can be classified into three patterns based on location (Nishibe et al. 2015). First, in the northern edge and around the axis of the first ridge of the KE, the bloom formation may be caused by the shoaling of the mixed layer through the intrusion of the warmer water from the south. Additionally, primary production and the contribution of large (>10 μm) phytoplankton to the total production (21–36%) was relatively high (Nishibe et al. 2015). The results at Stn. T3 (Fig. 9b) showed that the high phytoplankton biomass at the northern edge was dominated by diatoms. The prevalence of diatoms in this area in spring was also observed in previous microscopic studies (Marumo et al. 1961; Yamamoto et al. 1988). As mentioned above, a shallow MLD, caused by shoaling of the mixed layer through the intrusion of the warmer water from the south, would provide an environment advantageous to diatoms, which prefer high light conditions (Saito and Tsuda 2003). In addition, the diatom bloom would have been supported by a nutrient supply through upwelling (Allen et al. 2005), because the elevation of the nutricline was observed at Stn. T3 along the transect across the first ridge (Fig. S2a in the ESM), as suggested by Clayton et al. (2014). However, at Stn. T3, nitrate was depleted completely in the upper euphotic zone (refer to Fig. 3 in Nishibe et al. 2015). This implies that the diatom bloom at the northern edge of the first ridge will terminate due to the depletion of nutrients in the upper euphotic zone, resulting in lower primary production in the >10 μm fraction (Fig. 10). The decline of

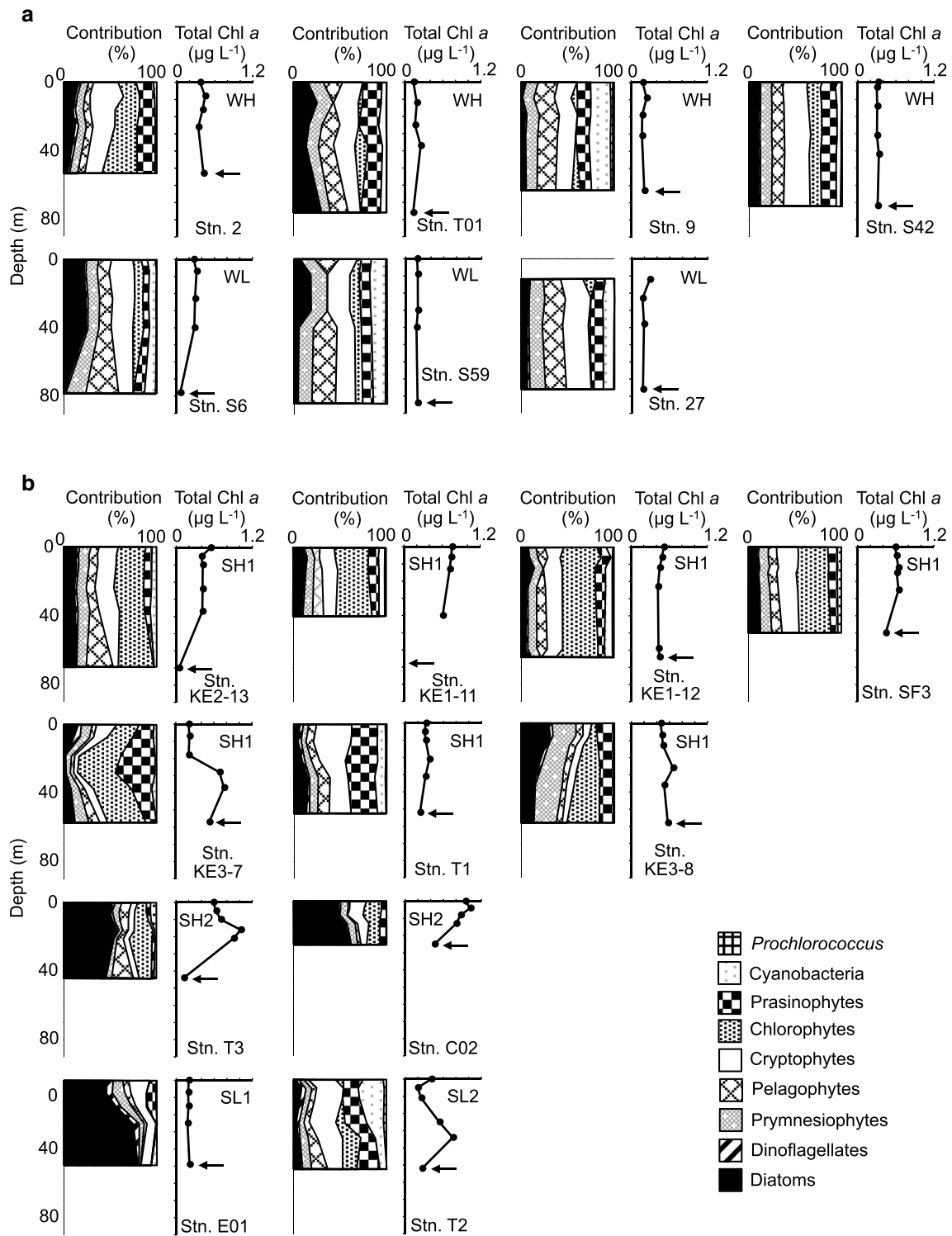


Fig. 9 Vertical structures of phytoplankton communities in the euphotic zone at stations where primary production was measured in the Kuroshio Extension and adjacent regions in **a** winter and **b** spring. The positions of *arrows* delineate the bottom of the euphotic zone

(1% light depth). The names of the phytoplankton community types at a depth of 10 m identified from the cluster analysis are superimposed on the subfigure for each station. The sites of these stations are shown in Fig. 1 of Nishibe et al. (2015)

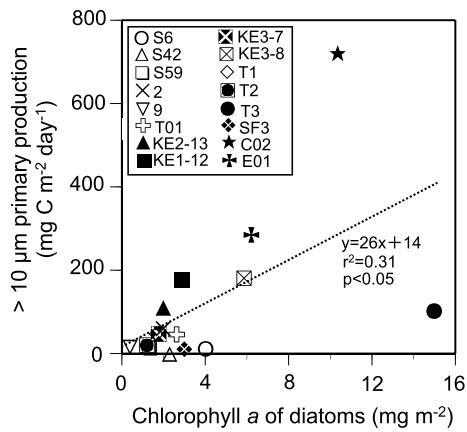


Fig. 10 Relationships between chlorophyll *a* of diatoms and >10 μm primary production in the euphotic zone at stations where primary production was measured (refer also to Table 1 in Nishibe et al. 2015). The dashed line is a regression line with a significant correlation between both parameters ($p < 0.05$, t test)

the bloom may be accelerated by the disproportionately high uptake of silicic acid by senescent diatoms in the decline phase of the bloom (Takeda 1998), since the silicic acid concentration at Stn. T3 was below $2 \mu\text{M}$, and cell division of diatoms generally ceases at such concentrations (Egge and Aksnes 1992). On the other hand, a community dominated by chlorophytes and cryptophytes was found near the axis of the first ridge (Stn. KE2-13) (Figs. 2b, 5a, 9b), which was characterised by a comparatively deep mixed layer (Nishibe et al. 2015) and no elevation of the nutricline (Fig. S2 in the ESM). A relatively high tolerance of cryptophytes to low light or nutrient availability has been inferred from cytological (Spear-Bernstein and Miller 1989) and field (Sato and Furuya 2010) studies. The results of an artificial upwelling experiment also support this, as nutrient enrichment into the bottom of the euphotic zone enhanced the growth of cryptophytes rather than that of diatoms (Masuda et al. 2010). Therefore, it is suggested that regional variations in light availability largely controlled by MLD in addition to the nutrient supply by upwelling help to drive the shift in the dominant algal taxon between diatoms and cryptophytes near the first ridge.

Second, in the south of the KE axis of the first ridge, both the total primary production and the contribution of large phytoplankton (12–31%) were high compared to those in the northern edge and around the axis of the first ridge, despite the deeper mixed layer in spring (Nishibe et al. 2015). Chlorophytes were suggested to be the main primary producers of and contributors to the bloom formation, because phytoplankton communities in the euphotic zone shifted from having no predominant phytoplankton taxa in winter (Stn. S6) to having chlorophytes as the dominant taxa in spring (Stns. KE1-11, KE1-12, and SF3)

(Fig. 9a, b). The predominance of chlorophytes probably occurs because of the high light utilisation efficiency of chlorophytes in low light conditions (Ryther 1956), and the growth of diatoms was constrained by a low silicic acid concentration during winter and spring (Nishibe et al. 2015). After the phytoplankton biomass decreased with the depletion of nitrate in late spring, cyanobacteria dominated, and the contribution from chlorophytes became low near to the sea surface (Figs. 2b, 5d; Table 3). A similar prevalence of cyanobacteria has also been observed in the south of the Kuroshio in the East China Sea (Furuya et al. 2003), and near the sea surface in the south of the KE front, where nitrate and nitrite concentrations were quite low (Clayton et al. 2014). Thus, the dominance of cyanobacteria in conjunction with nitrate depletion is thought to be a typical feature south of the KE after the spring bloom.

Third, to the east of the first ridge, primary production and the contribution of large phytoplankton to total production (7–15%) were lower than they were in the vicinity of the first ridge (Nishibe et al. 2015). Primary productivity was strongly affected by advection, which causes upward and downward transport of nutrients and phytoplankton resulted from the cross-frontal flow along the meander of the KE (Ito et al. 2000). A distinct SCM was formed near the first trough (Stns. T2 and KE 3-7), reflecting the downward advection from the first ridge to the first trough along the meander of the KE (Bower 1991; Ito et al. 2000) in addition to nutrient consumption in the upper euphotic zones (Fig. 4 in Nishibe et al. 2015). In spring, at the northern edge of the first trough (Stn. T2), cryptophytes were the most important primary producers, followed by prasinophytes and chlorophytes, while chlorophytes were the most important, followed by prasinophytes, at a station in the south of the first trough (Stn. KE3-7) (Fig. 9b). In the south of the first trough, the dominance of chlorophytes increased from winter (Stn. S59) to spring (Stn. KE3-7), suggesting that chlorophytes were the main contributors to the formation of the spring bloom, just as they were in the south of the first ridge (Fig. 9a, b). In contrast, phytoplankton biomass was highest in the upper part of the euphotic zone, and was dominated by cryptophytes and prasinophytes at the northern edge of the second ridge (Stn. T1) (Fig. 9b), probably due to the upward advection from the first trough to the second ridge (Bower 1991; Ito et al. 2000). A relatively low abundance of diatoms and low primary production (both total production and that of the >10 μm fraction) occurred at Stn. T1, despite a shallow MLD and high concentrations of nitrate and silicic acid (Nishibe et al. 2015). This could be explained by iron limitation (Shiozaki et al. 2014). Similarly, the high abundance of diatoms found in Stn. T3 may be partly explained by the iron supplied by the iron-rich North Pacific Intermediate Water (Nishioka et al. 2007) that is transported southwards along the continental

shelf (Yasuda 2003). This is in accordance with the results of field observations in the Peru upwelling, in which cryptophytes and prasinophytes prevailed in the low-iron area, where the growth of diatoms was suppressed (DiTullio et al. 2005). In contrast, it was interesting that diatoms were observed to dominate in the transition region just north of the second ridge (Stn. K1) along 149°E (Figs. 2b, 5d). This can probably be attributed to the advection of coastal diatom species from the west (Marumo 1967; Yamamoto et al. 1988). To understand the factors affecting the distribution and production of diatoms near the second ridge, it will be necessary to identify and estimate the growth of diatoms and to determine the iron concentration.

This study confirmed that the main components >10 µm in the study sites were diatoms, since a significant positive correlation was only observed between biomass of diatoms and chlorophyll *a* in the >10 µm fraction ($p < 0.05$, *t* test, data not shown). However, it is noteworthy that, other than at Stn. T3 (where diatoms were predominant), a relatively high primary production in the >10 µm fraction was observed at some stations where diatoms did not dominate (Stns. KE1-12 and KE2-13) (Figs. 9b, 10). Some cryptophyte and prymnesiophyte species reported from the KE, the Kuroshio and Sagami Bay, including *Teleaulax* spp., *Geminigera* spp. (Kok et al. 2014), *Calcidiscus leptoporus*, *Chrysochromulina ephippium*, *Chrysochromulina* spp., *Helicosphaera carteri*, *Umbilicosphaera sibogae*, *Chroomonas* sp., *Leucocryptos marina* and *Teleaulax acuta* (Thronsen 1983), are known to exceed 10 µm in cell size. These >10 µm non-diatom phytoplankton may have contributed to the primary production in the >10 µm fraction in the KE region.

This study showed that during the spring bloom, phytoplankton communities in the KE region are generally composed of small phytoplankton groups such as chlorophytes, cryptophytes, and prasinophytes. However, a predominance of diatoms occurs locally at the temperature front near the first ridge of the KE in spring, where high biomass and the production of nauplii and small copepods were reported (Nakata et al. 1995). Since copepods generally prefer to prey on >10 µm phytoplankton (Runge 1980), the temperature front near the first ridge was suggested to be a key area for the recruitment success of pelagic fishes in the KE region. Our results indicate that fluctuations of the flow path of the KE could influence not only the biomass (Nishibe et al. 2015) but also the compositions of the phytoplankton communities during the succession of the spring bloom. For instance, the uniform distribution of communities dominated by chlorophytes, followed by cryptophytes, throughout the KE region in April 2008 may have resulted from the active water-mass changes between the south and the north of the KE because of the unstable mode of the KE (Qiu and Chen 2005). This unstable

KE mode, which prevents the formation of a stable front structure, may hinder intensive diatom bloom formation (such as that seen in May 2009), and this may have adverse effects on the grazing food chain. However, some copepods are known to selectively graze nanophytoplankton rather than microphytoplankton (Calbet et al. 2000). On the other hand, some non-diatom groups such as cryptophytes and prymnesiophytes, which dominated in the communities near the KE, include species larger than 10 µm. Therefore, it is necessary to identify the prey–predator relationships in the planktonic food web, particularly those related to the predominant non-diatom prey, in order to accurately evaluate the importance of the Kuroshio Extension as a nursery area for pelagic fish larvae.

Acknowledgements We thank the captains, crews, and scientists on board the cruises of the R/V *Wakataka-Maru*, R/V *Shoyo-Maru*, R/V *Hakuho-Maru*, and R/V *Tansei-Maru* for their cooperation at sea. We also thank Dr. M. Nakamachi and Dr. T. Ikeya for nutrient data, and Dr. X. Liu and Dr. M. Iwataki for their helpful suggestions regarding the pigment analysis. This study was financially supported by the grant “Studies on Prediction and Application of Fish Species Alternation” (SUPRFISH) from the Research Development of Agriculture, Forestry, and Fisheries Research Council as well as a MEXT grant (24121005).

References

- Allen JT, Brown L, Sanders R, Moore CM, Mustard A, Fielding S, Lucas M, Rixen M, Savidge G, Henson S, Mayor D (2005) Diatom carbon export enhanced by silicate upwelling in the northeast Atlantic. *Nature* 437:728–732
- Bower AS (1991) A simple kinematic mechanism for mixing fluid parcels across a meandering jet. *J Phys Oceanogr* 21:173–180
- Calbet A, Landry MR, Scheinberg RD (2000) Copepod grazing in a subtropical bay: species-specific responses to a midsummer increase in nanoplankton standing stock. *Mar Ecol Prog Ser* 193:75–84
- Clarke KR, Gorley RN (2006) PRIMER v6: user manual/tutorial. PRIMER-E, Plymouth
- Clayton S, Nagai T, Follows MJ (2014) Fine scale phytoplankton community structure across the Kuroshio Front. *J Plankton Res* 36:1017–1030
- Clayton S, Lin YC, Follows MJ, Worden AZ (2017) Co-existence of distinct *Ostreococcus* ecotypes at an ocean front. *Limnol Oceanogr* 62:75–88
- DiTullio GR, Geesey ME, Maucher JM, Alm MB, Riseman SF (2005) Influence of iron on algal community composition and physiological status in the Peru upwelling system. *Limnol Oceanogr* 50:1887–1907
- Egge JK, Aksnes DL (1992) Silicate as regulating nutrient in phytoplankton competition. *Mar Ecol Prog Ser* 83:281–289
- Furuya K, Hayashi M, Yabushita Y, Ishikawa A (2003) Phytoplankton dynamics in the East China Sea in spring and summer as revealed by HPLC-derived pigment signatures. *Deep-Sea Res II* 50:367–387
- Hansen HP, Koroleff F (1999) Determination of nutrients. In: Grasshoff K, Kremling K, Ehrhardt M (eds) *Methods of seawater analysis*, 3rd edn. Wiley-VCH, Weinheim, pp 159–228

- Hashihama F, Horimoto N, Kanda J, Furuya K, Ishimaru T, Saino T (2008) Temporal variation in phytoplankton composition related to water mass properties in the central part of Sagami Bay. *J Oceanogr* 64:23–37
- Isada T, Kuwata A, Saito H, Ono T, Ishii M, Yoshikawa-Inoue H, Suzuki K (2009) Photosynthetic features and primary productivity of phytoplankton in the Oyashio and Kuroshio–Oyashio transition regions of the northwest Pacific. *J Plankton Res* 31:1009–1025
- Ito S, Matsuo Y, Yokouchi K, Inagake D (2000) Cross frontal flow associated with meanders of the Kuroshio Extension and distribution of chlorophyll-*a*. *Bull Tohoku Natl Fish Res Inst* 63:125–134
- Kawai H (1972) Hydrography of the Kuroshio Extension. In: Stommel H, Yoshida K (eds) *Kuroshio—its physical aspects*. University of Tokyo Press, Tokyo, pp 235–354
- Kawarada Y, Kito M, Furuhashi K, Sano A (1968) Distribution of plankton in the waters neighboring Japan in 1966 (CSK). *Oceanogr Mag* 20:187–212
- Kok SP, Kikuchi T, Toda T, Kurosawa N (2012a) Diversity analysis of protistan microplankton in Sagami Bay by 18S rRNA gene clone analysis using newly designed PCR primers. *J Oceanogr* 68:599–613
- Kok SP, Kikuchi T, Toda T, Kurosawa N (2012b) Diversity and community dynamics of protistan microplankton in Sagami Bay revealed by 18S rRNA gene clone analysis. *Plankton Benthos Res* 7:75–86
- Kok SP, Tsuchiya K, Komatsu K, Toda T, Kurosawa N (2014) The protistan microplankton community along the Kuroshio current revealed by 18S rRNA gene clone analysis: a case study of the differences in distribution interplay with ecological variability. *Plankton Benthos Res* 9:71–82
- Latasa M (2007) Improving estimations of phytoplankton class abundances using CHEMTAX. *Mar Ecol Prog Ser* 329:13–21
- Levitus S (1982) Climatological atlas of the world ocean. NOAA Prof Pap 13, US Govt Printing Office, Washington, DC
- Mackey MD, Mackey DJ, Higgins HW, Wright SW (1996) CHEMTAX—a program for estimating class abundances from chemical markers: application to HPLC measurements of phytoplankton. *Mar Ecol Prog Ser* 144:265–283
- Mackey DJ, Higgins HW, Mackey MD, Holdsworth D (1998) Algal class abundances in the western equatorial Pacific: estimation from HPLC measurements of chloroplast pigments using CHEMTAX. *Deep-Sea Res I* 45:1441–1468
- Marumo R (1967) General features of diatom communities in the North Pacific Ocean in summer. *Inf Bull Planktol Japan* 115–121
- Marumo R, Asaoka O, Karoji K (1961) On the distribution of *Eucampia zoodiacus* Ehrenberg with reference to hydrographic conditions. *J Oceanogr* 17:45–47
- Masuda T, Furuya K, Kohashi N, Sato M, Takeda S, Uchiyama M, Horimoto N, Ishimaru T (2010) Langrangian observation of phytoplankton dynamics at an artificially enriched subsurface water in Sagami Bay, Japan. *J Oceanogr* 66:801–813
- Miki M, Ramaiah N, Takeda S, Furuya K (2008) Phytoplankton dynamics associated with the monsoon in the Sulu Sea revealed by pigment signature. *J Oceanogr* 64:663–673
- Nakata K (1988) Alimentary tract contents and feeding conditions of ocean-caught post larval Japanese sardine, *Sardinops melanostictus*. *Bull Tokai Reg Fish Res Lab* 126:11–24
- Nakata K, Zenitani H, Inagake D (1995) Differences in food availability for Japanese sardine larvae between the frontal region and the waters on the offshore side of the Kuroshio. *Fish Oceanogr* 4:68–79
- Nishibe Y, Takahashi K, Shiozaki T, Kakehi S, Saito H, Furuya K (2015) Size-fractionated primary production in the Kuroshio extension and adjacent regions in spring. *J Oceanogr* 71:27–40
- Nishioka J, Ono T, Saito H, Nakatsuka T, Takeda S, Yoshimura T, Suzuki K, Kuma K, Nakabayashi S, Tsumune D, Mitsudera H, Johnson WK, Tsuda A (2007) Iron supply to the western subarctic Pacific: importance of iron export from the Sea of Okhotsk. *J Geophys Res* 112:C10012
- Noto M, Yasuda I (2003) Empirical biomass model for the Japanese sardine, *Sardinops melanostictus*, with sea surface temperature in the Kuroshio Extension. *Fish Oceanogr* 12:1–9
- Odate T, Maita Y (1988) Regional variation in the size composition of phytoplankton communities in the western North Pacific Ocean, spring 1985. *Biol Oceanogr* 6:65–77
- Qiu B, Chen S (2005) Variability of the Kuroshio Extension jet, recirculation gyre, and mesoscale eddies on decadal time scales. *J Phys Oceanogr* 35:2090–2103
- Roy S, Llewellyn CA, Egeland ES, Johnsen G (2011) Phytoplankton pigments: characterization, chemotaxonomy and applications in oceanography. Cambridge University Press, Cambridge, pp 257–313
- Runge JA (1980) Effects of hunger and season on the feeding behavior of *Calanus pacificus*. *Limnol Oceanogr* 25:134–145
- Ryther JH (1956) Photosynthesis in the ocean as a function of light intensity. *Limnol Oceanogr* 1:61–70
- Saito H, Tsuda A (2003) Influence of light intensity on diatom physiology and nutrient dynamics in the Oyashio region. *Prog Oceanogr* 57:251–263
- Sato M, Furuya K (2010) Pico- and nanophytoplankton dynamics during the decline phase of the spring bloom in the Oyashio region. *Deep Sea Res II* 57:1643–1652
- Shiozaki T, Ito S, Takahashi K, Saito H, Nagata T, Furuya K (2014) Regional variability of factors controlling the onset timing and magnitude of spring algal blooms in the northwestern North Pacific. *J Geophys Res C* 119:253–265
- Spear-Bernstein L, Miller KR (1989) Unique location of the phycoliprotein light-harvesting pigment in the cryptophyceae. *J Phycol* 25:412–419
- Takahashi M, Nishida H, Yatsu A, Watanabe Y (2008) Year-class strength and growth rates after metamorphosis of Japanese sardine (*Sardinops melanostictus*) in the western North Pacific Ocean during 1996–2003. *Can J Fish Aquat Sci* 65:1425–1434
- Takasuka A, Oozeki Y, Aoki I (2007) Optimal growth temperature hypothesis: why do anchovy flourish and sardine collapse or vice versa under the same ocean regime? *Can J Fish Aquat Sci* 64:768–776
- Takeda S (1998) Influence of iron availability on nutrient consumption ratio of diatoms in oceanic waters. *Nature* 393:774–777
- Thronsen J (1983) Ultra- and nanoplankton flagellates from coastal waters of southern Honshu and Kyushu, Japan (including some results from the western part of the Kuroshio off Honshu). Working Party on Taxonomy in the Akashiwo Mondai Kenkyukai Fishing Ground Preservation Division. Research Department, Fisheries Agency, Tokyo, pp 1–62
- Watanabe Y (2007) Latitudinal variation in the recruitment dynamics of small pelagic fishes in the western North Pacific. *J Sea Res* 58:46–58
- Yamamoto T, Nishizawa S, Taniguchi A (1988) Formation and retention mechanisms of phytoplankton peak abundance in the Kuroshio front. *J Plankton Res* 10:1113–1130
- Yasuda I (2003) Hydrographic structure and variability in the Kuroshio–Oyashio Transition Area. *J Oceanogr* 59:389–402
- Yatsu A, Watanabe T, Ishida M, Sugisaki H, Jacobson LD (2005) Environmental effects on recruitment and productivity of Japanese sardine *Sardinops melanostictus* and chub mackerel *Scomber japonicus* with recommendation for management. *Fish Oceanogr* 14:263–278
- Zapata M, Rodriguez F, Garrido JL (2000) Separation of chlorophylls and carotenoids from marine phytoplankton: a new HPLC method using a reversed phase C₈ column and pyridine-containing mobile phases. *Mar Ecol Prog Ser* 195:29–45